Reaction Kinetics Modeling and Thermal Properties of Epoxy–Amines as Measured by Modulated-Temperature DSC. I. Linear Step-Growth Polymerization of DGEBA + Aniline

Steven Swier, Guy Van Assche, Bruno Van Mele

Department of Physical Chemistry and Polymer Science, Vrije Universiteit Brussel (VUB), Pleinlaan 2, B-1050 Brussels, Belgium

Received 3 February 2003; accepted 29 July 2003

ABSTRACT: A mechanistic approach including both reactive and nonreactive complexes can successfully simulate both nonreversing (NR) heat flow and heat capacity (C_p) signals from modulated-temperature DSC in isothermal and nonisothermal reaction conditions for different mixtures of diglycidyl ether of bisphenol A + aniline. The reaction of the primary amine with an epoxy–amine complex initiates cure (E_{1A1} = 80 kJ mol^{-1}), whereas the reactions of the primary amine (E_{1OH} = 48 kJ mol^{-1}) and secondary amine (E_{2OH} = 48 kJ mol^{-1}) with an epoxy–hydroxyl complex are rate determining from about 2% epoxy conversion on. The reliability of the proposed mechanistic model was verified by experimental concentration profiles from Raman spectroscopy. When cure temperatures are chosen inside or below the full cure glass-transition region, vitrification takes place partially or completely, respectively, as can be concluded from the magnitude of the stepwise decrease in C_p. The effect of the epoxy conversion (x) and mixture composition on thermal properties such as the glass-transition temperature (T_g), the change in heat capacity at T_g [$\Delta C_p(T_g)$], and the width of the glass transition region (ΔT_g) are considered. The Couchman relationship, in which only T_g and $\Delta C_p(T_g)$ of both the unreacted and the fully reacted systems are needed, was evaluated to predict the T_g– x relation by using simulated concentration profiles. © 2004 Wiley Periodicals, Inc. J Appl Polym Sci 91: 2798–2813, 2004

Key words: modulated-temperature differential scanning calorimetry (MTDSC); step-growth polymerization; kinetics (polym.); modeling; thermoset

INTRODUCTION

To characterize and optimize the curing behavior of commercial thermosetting networks, the (epoxy) conversion (x) and its influence on the (thermal) properties are of interest.[1] To simulate changes in thermal properties for a certain imposed cure schedule, the relation between the conversion and the cure temperature (T_{cure})/time (t) has to be known. Although empirical approaches relating the global conversion of epoxide groups to the overall conversion rate can be used to simulate the effect of T_{cure} on the reaction rate and thus x, they are specific to a certain chemistry and composition.[2,3] A mechanistic approach based on the influence of both reactive and nonreactive complexes on the primary amine–epoxy and secondary amine–epoxy reaction step was able to simulate isothermal and nonisothermal experiments for a wide range of mixture compositions from modulated-temperature DSC (MTDSC) and concentration profiles obtained from high-performance liquid chromatography (HPLC).[4] The simultaneously obtained nonreversing heat flow, providing the (global) epoxy conversion, and the heat capacity signal, providing specific information on both amine–epoxy reactions,[5] turns out to be beneficial for optimizing the kinetic parameters. Moreover, the concentration profiles obtained from HPLC are not needed to obtain this optimized set for the model epoxy–amine system phenyl glycidyl ether (PGE) + aniline. The applicability of this approach will be tested here for the linearly polymerizing system diglycidyl ether of bisphenol A (DGEBA) + aniline. Raman spectroscopy will be used to check the validity of the simulated concentration profiles.

Thermal properties such as the glass-transition temperature (T_g), the change in heat capacity at the glass transition [$\Delta C_p(T_g)$], and the width of the glass-transition region (ΔT_g) can be readily obtained from DSC analysis.[6] Their evolution with x will shed more light on the drastic changes that occur during cure, transforming a low molecular weight reactive liquid into a polymeric glass. MTDSC will be used in this respect to analyze the thermal properties as a function of x in nonisothermal experiments following the preceding

Correspondence to: B. Van Mele (bvmele@vub.ac.be).

Contract grant sponsor: Flemish Institute for the Promotion of Scientific-Technological Research in Industry (I.W.T.).

Journal of Applied Polymer Science, Vol. 91, 2798–2813 (2004)

cure schedule. The benefits of MTDSC over conventional DSC relate to the deconvolution of T_g and $\Delta C_p(T_g)$ from the (residual) heat of reaction in the heat capacity and nonreversing heat flow signals, respectively.[7] Moreover, because the former signal is solely obtained from the cyclic response to the modulated temperature input, most noise and baseline effects are found only in the latter signal.[8] The evolution of $\Delta C_p(T_g)$ with x, from ΔC_{p0} (unreacted) to $\Delta C_{p\text{full}}$ (fully cured), relates to differences in molecular motions between the glassy and "liquid" state of the evolving polymer chain.[9]

The relation between T_g and x, especially in comparison to T_{cure}, is important in view of the transition from chemically controlled to diffusion-controlled reaction[10] (see also second part of this series[11]). A model based on thermodynamic considerations was initially presented by Couchman to calculate the T_g of polymer blends.[12] This approach can be extended to reactive systems by assuming that the system at conversion x consists of a random mixture of unreacted segments with fraction $1 - x$ and associated $T_g = T_{g0}$ and reacted segments with fraction x and associated $T_g = T_{g\text{full}}$[13]:

$$\ln(T_g) = \frac{(1-x)\ln(T_{g0}) + \dfrac{\Delta C_{p\text{full}}}{\Delta C_{p0}}\, x \ln(T_{g\text{full}})}{(1-x) + \dfrac{\Delta C_{p\text{full}}}{\Delta C_{p0}}\, x} \qquad (1)$$

where $\Delta C_{p0} = \Delta C_p(T_g = T_{g0})$ and $\Delta C_{p\text{full}} = \Delta C_p(T_g = T_{g\text{full}})$. This equation can predict the evolution of T_g with x for several thermosetting network-forming and linear systems.[13] The validity of this relation for the DGEBA + aniline system will be investigated in view of the information (concentration profiles) obtained from the mechanistic model.

EXPERIMENTAL

Materials

The bifunctional epoxy diglycidyl ether of bisphenol A (DGEBA, $f = 2$) was obtained from Shell (Houston, TX) as the high-purity Epon™ Resin 825. A single molecular structure is reported for the epoxy, whereas a low molecular weight component is added to reduce the viscosity [epoxy equivalent weight (EEW) = 180 g/mol].[14] Aniline ($f = 2$, $M_w = 93$ g/mol, purity = 99%) was obtained from Aldrich (Milwaukee, WI). Both components were used without further purification and mixed in the appropriate quantities at room temperature.

A GPC analysis (see section on gel permeation chromatography, below) on the Epon Resin 825 reveals a small fraction (<5%) of a low molecular weight material. No high molecular weight shoulder was detected, confirming that n is close to zero so that the initial hydroxyl concentration is negligible:

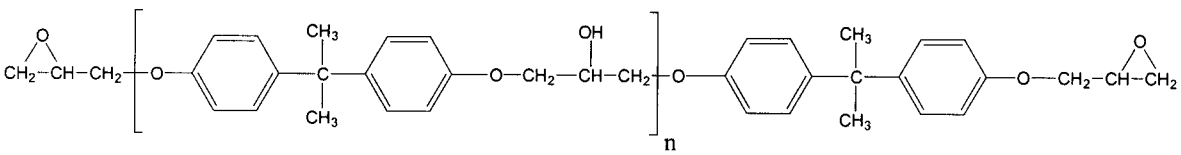

DGEBA (Epon™ Resin 825: $n \rightarrow 0$)

The low molecular weight material, causing an increase in EEW from 170 g/mol (corresponding to $n = 0$) to 180 g/mol in Epon 825, is considered to be an inert additive. If additional epoxide functionalities would be present (which cannot be excluded), it is assumed they have the same reactivity as those of the main component (see section on optimized parameters, below).

Modulated-temperature DSC

The TA Instruments 2920 DSC (TA Instruments, New Castle, DE) with MDSC™ option and a refrigerated cooling system (RCS) was used for MTDSC measurements. Samples ranging from 5 to 10 mg were measured using hermetic crucibles. Helium was used as a purge gas (25 mL/min). Indium and cyclohexane were used for temperature and enthalpy calibration. Heat capacity calibration was performed with a poly(methyl methacrylate) (PMMA) standard (supplied by Acros, Geel, Belgium), using the heat capacity difference between two temperatures (one above and one below the glass-transition temperature of PMMA[15]) to ensure that heat capacity changes were adequately measured. Quasi-isothermal measurements were performed using a modulation amplitude of 1°C in combination with a period of 60 s. For quantitative heat capacity measurements at temperatures below −50°C, a temperature-dependent C_p calibration was used. This consisted of measuring the heat capacity evolution of a reference material (sapphire) over the whole temperature range of interest and calculating a heat capacity calibration factor as a function of temperature.[16]

FT-Raman spectroscopy

Raman spectrometry measurements were performed on a Perkin–Elmer System 2000 FTIR spectrometer (Perkin Elmer Cetus Instruments, Norwalk, CT) equipped with a System 2000R FT-Raman accessory. The measurements were performed with back-scattering (180°) collection using a quartz beamsplitter and an InGaAs detector. Approximately 2 mg of the fresh DGEBA + aniline sample was introduced into a 1 mm thick glass capillary, which was subsequently sealed with a butane/oxygen burner while protecting the sample under liquid nitrogen. A hermetic seal was obtained in this way, whereas no preliminary epoxy–amine reaction occurred. The capillary was then cured in a cylindrical aluminum holder in the 2920 DSC cell to make sure that measurements from MTDSC and FT-Raman underwent the same cure schedule. Moreover, the thin glass capillaries reduced thermal gradients inside the sample. Spectra were recorded at a resolution of 4 cm^{-1} using a laser power of 600 mW, accumulating 36 scans.

Gel permeation chromatography (GPC)

The weight-average molecular weights and the molecular weight distributions were determined using a Waters 2690 Alliance gel permeation chromatograph (Waters Chromatography Division/Millipore, Milford, MA) equipped with two Styragel HR 5E columns, a Waters 410 differential refractometer, and a Viscotek T50A differential viscometer (Viscotek, Houston, TX). The eluent used was tetrahydrofuran (THF). Absolute molecular weights were calculated by performing a universal calibration using polystyrene standards.

RESULTS AND DISCUSSION

Mechanistic model

Reaction mechanism

In comparison to a kinetic study of the model system PGE + aniline forming a low molecular weight compound,[4] an assumption has to be made here to be able to use the same reaction steps. Flory proposed the principle of equal reactivity of functional groups, stating that the reactivity of functional groups can be expected to be independent of molecular size and thus unaffected by the reaction of the other functional group(s) in the molecule or monomer from which it is derived.[17] This, for example, means that the reactivity of the functional groups—epoxy (E), primary amine (A_1), and secondary amine (A_2)—in the linear step-growth polymerization of DGEBA + aniline can be considered to be independent of the molecular weight. The mechanism used for the model epoxy–amine PGE + aniline[4] will be applied to the DGEBA + aniline system. In this way, the specificity of the proposed reaction steps can be tested,[18,19] as shown in Scheme 1:

Reactive complexes:

$E + Cat \rightleftharpoons ECAT$ $\quad K_{ECat}$

Primary and secondary amine-epoxy reaction:

$ECat + A_1 \rightarrow OH + A_2 + Cat$ $\quad k_{1Cat}(A_{1Cat}, E_{1Cat})$

$ECat + A_2 \rightarrow OH + A_3 + Cat$ $\quad k_{2Cat}(A_{2Cat}, E_{2Cat})$

Non reactive complexes:

$A_1 + OH \rightleftharpoons A_1OH$ $\quad K_{A1OH}$

$Et + OH \rightleftharpoons EtOH$ $\quad K_{EtOH}$

$Et + A_1 \rightleftharpoons EtA_1$ $\quad K_{EtA1}$

Scheme 1

where E is the epoxide group; A_1, A_2, and A_3 are the primary, secondary, and tertiary amine groups, respectively; OH is the hydroxyl group formed during the reaction; Cat designates catalysts OH and A_1; ECat is an equilibrium complex; and Et is the ether group of the epoxy. The notation for the equilibrium constant (K) and reaction rate constants (k) with their respective activation energies (E) and preexponential factors (A) are also given. Apart from the reactive complexes (EOH and EA_1) that cause an acceleration, the presence of nonreactive complexes will decrease the reaction rate.

Experimental input

Concentrations of reactive groups as determined by FT-Raman. Samples of stoichiometric DGEBA + aniline mixtures were cured at 100°C in glass capillaries for different times. The Raman spectra taken at different cure times are overlaid in Figure 1. All obtained spectra were normalized using the reference band corresponding to the vibration of the *para*-disubstituted phenyl band of DGEBA at 1114 cm^{-1}.[20,21] To calculate the concentration of epoxy functionalities, the band at 1260 cm^{-1} was used, which is attributed to ring breathing of the epoxy ring. The band at 1230 cm^{-1} associated with the aromatic ether stretch partly overlaps with the epoxy band and was deconvoluted using Gaussian peaks to quantify the evolution of the epoxy concentration. The skeletal vibration of the mono-substituted aromatic ring associated with the amine (aniline: 997 cm^{-1}) was used to resolve the concentrations of the amine functionalities.[22] This is based on the change in Raman shift with the amine substitution: the Raman wavenumber shifts to lower values in the series primary amine (A_1), secondary amine (A_2), and tertiary amine (A_3).[23] The skeletal vibration band of

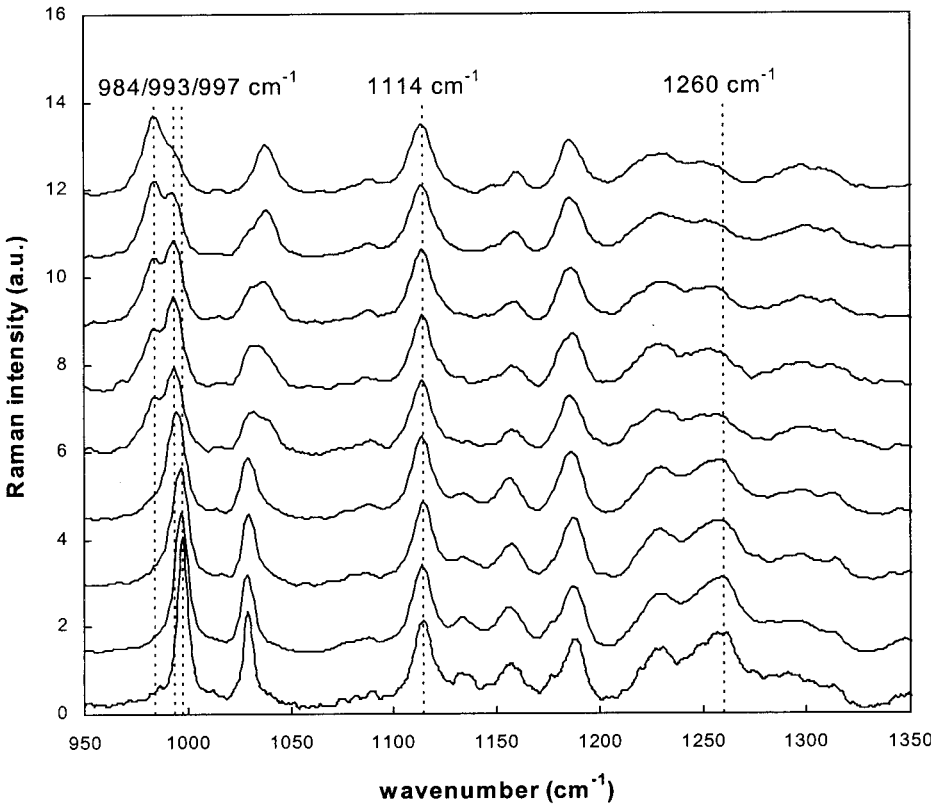

Figure 1 Raman spectra of a stoichiometric DGEBA + aniline mixture cured at 100°C for different times (from bottom to top): 0, 21, 46, 62, 80, 100, 115, 145, and 300 min; the band positions used in this work are indicated with their Raman shifts; spectra were normalized using the reference band at 1114 cm^{-1}.

model compounds based on aniline, for which one or two hydrogen atoms were substituted for methyl and ethyl groups, was analyzed for reference: *N*-methylaniline (992 cm^{-1}), *N*-ethylaniline (994 cm^{-1}), and *N,N*-diethylaniline (987 cm^{-1}). The following Raman shifts were taken for the amines formed during DGEBA + aniline cure (see also Fig. 1): 997 cm^{-1} for A_1, 993 cm^{-1} for A_2, and 984 cm^{-1} for A_3.

The region associated with these amine absorptions was also deconvoluted using Gaussian peaks to determine the evolution of their concentrations. The concentration profiles obtained for all reactive functionalities are shown below (see simulation of experimental trends).

Heat flow and heat capacity from MTDSC: link with the concentration profiles. An equal reaction enthalpy was found for the primary amine and secondary amine–epoxy reaction step of the model system PGE + aniline,[5] which could be extended to other glycidyl type epoxies like DGEBA. The heat flow signal (d_rH/dt) is therefore directly related to the conversion rate of epoxide groups (dx/dt):

$$\frac{d_rH}{dt} = \frac{dx}{dt}\,\Delta_rH \tag{2}$$

with $x(t) = ([E]_0 - [E])/[E]_0$ or by integration to time t:

$$\Delta_rH(t) = x(t)\Delta_rH \tag{3}$$

where $[E]_0$ and $[E]$ are the concentration of epoxide groups at times 0 and t, respectively; x is the epoxy conversion; and Δ_rH is the reaction enthalpy. Note that Δ_rH corresponds to the total reaction enthalpy (all epoxide groups are converted), whereas $\Delta_rH(t)$ designates the partial reaction exothermicity until time t [corresponding to $x(t)$]. The effect of cure temperature on this value is negligible.[5] Experimental confirmation of eq. (3) is given in Figure 2, which plots the reaction exothermicity obtained from the nonreversing heat flow signal as a function of the conversion obtained from the epoxy band in FT-Raman (see also the section on simulation of experimental trends, below).

Although a global conversion can be obtained from the heat flow signal, resolved information is available in the heat capacity signal because the primary and secondary amine–epoxy reaction steps contribute differently to the reaction heat capacity (in J mol^{-1} K^{-1})[5]:

$$\Delta_rC_{p,\text{prim}} = a + 0.018(T_{\text{cure}} - 298.15) - 0.00085(T_{\text{cure}} - 298.15)^2$$
$$\Delta_rC_{p,\text{sec}} = b + 0.35(T_{\text{cure}} - 298.15) - 0.00024(T_{\text{cure}} - 298.15)^2 \tag{4}$$

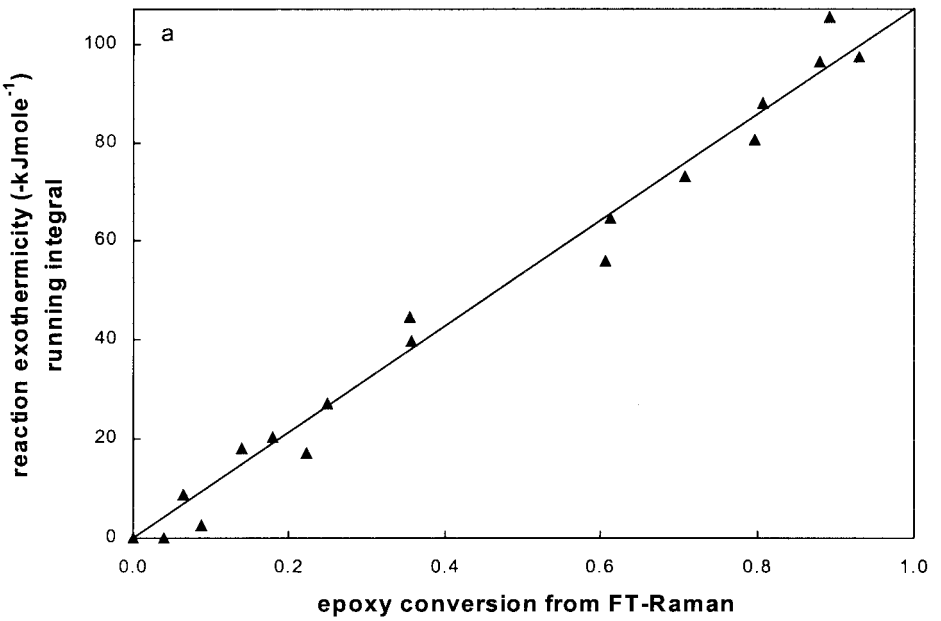

Figure 2 Running integral of the reaction exothermicity [$\Delta_r H(t)$] as a function of the epoxy conversion as obtained from FT-Raman spectra for DGEBA + aniline cured at 100°C for different times (▲); the fit to eq. (3) (—) results in $\Delta_r H = -107$ kJ mol^{-1}.

where $a = 16.1$ J mol^{-1} K^{-1}, $b = 12.6$ J mol^{-1} K^{-1}, and T_{cure} is in K.

Equation (4) was obtained for the model PGE + aniline system and allowed the simulation of heat capacity trends from MTDSC experiments at different cure temperatures and for different mixture compositions.[4] This equation will be used as a starting point for DGEBA + aniline as explained in the next section (optimization strategy).

To link $\Delta_r C_{p,\text{prim}}$ and $\Delta_r C_{p,\text{sec}}$ from equation 4 with the heat capacity changes obtained experimentally with MTDSC, the concentration profiles as calculated in the optimization program will be used:

$$\Delta_r C_p = \Delta_r C_{p,\text{prim}}([A_2] + [A_3]) + \Delta_r C_{p,\text{sec}}[A_3] \qquad (5)$$

where $[A_i]$ concentrations are in mol kg^{-1}, $\Delta_r C_{p,\text{prim}}$ and $\Delta_r C_{p,\text{sec}}$ are in J mol^{-1} K^{-1}, and $\Delta_r C_p$ is in J kg^{-1} K^{-1}.

Reaction kinetics

Initial reaction rate. The initial consumption rate of epoxide groups can be used to validate the initial reaction rate as proposed by the reaction scheme discussed earlier:

$$-\left.\frac{d[E]}{dt}\right|_0 = k_{1A1}[EA_1]_0[A_1]_0 = k'_{1A1}[E]_0[A_1]_0^2 \qquad (6)$$

where $k_{1A1} = k_{1A1}K_{1A1}$.[4]

Equation (2) can be used to obtain this consumption rate experimentally from the heat flow at $t = 0$ $(d_r H/dt)_0$:

$$-\left.\frac{d[E]}{dt}\right|_0 \frac{1}{[E]_0} = \left.\frac{dx}{dt}\right|_0 = \left.\frac{d_r H}{dt}\right|_0 \frac{1}{\Delta_r H} \qquad (7)$$

The reaction enthalpy $\Delta_r H$ corresponds to the total reaction exothermicity per mole of epoxide groups equaling -107 kJ mol^{-1} on average for the DGEBA + aniline system. The normalized epoxy consumption rate [see eq. (7)] is plotted as a function of the initial primary amine concentration in Figure 3. The order in A_1 for cure temperatures of 100 and 110°C is close to 2 as predicted by eq. (6) (see also the section on reaction mechanism).

Optimization strategy. The nonreversing heat flow signal (in both isothermal and nonisothermal conditions) and the change in heat capacity (in isothermal conditions) were used as input signals for mechanistic modeling. The validity of the optimized kinetic parameters in a wide temperature range was ensured by combining nonisothermal experiments with heating rates from 0.5 to 2.5°C/min with isothermal experiments from 60 to 110°C. Data points were considered in the chemically controlled region only and corresponded to the region before the onset of the relaxation peak in the heat flow phase[24] (elaborated in the second part of this series[11]). The mixture composition (r = mol NH/mol epoxide) was varied from 0.39 to 1.30, a range corresponding to initial concentrations of DGEBA and

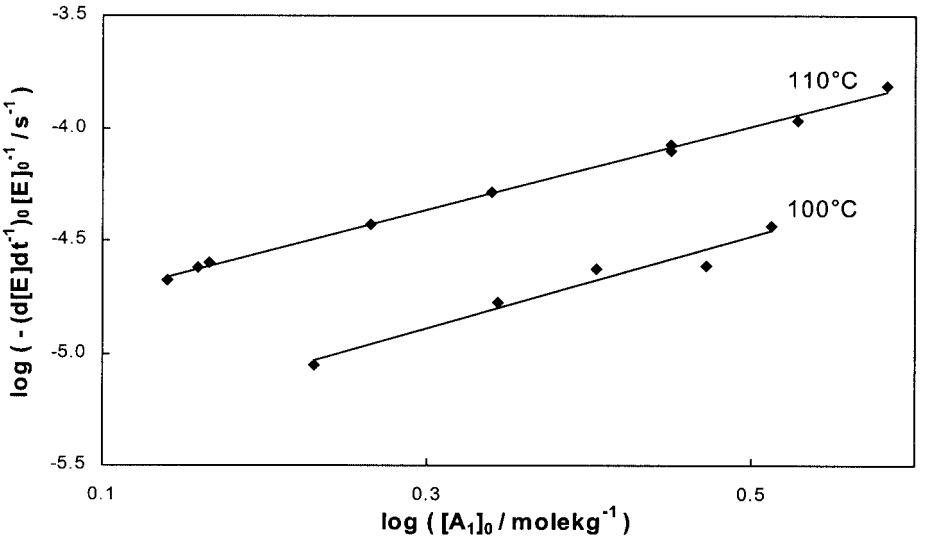

Figure 3 Conversion rate of epoxide groups at $t = 0$ as calculated from the nonreversing heat flow signal as a function of initial concentration of primary amine groups (◆) at 100 and 110°C (log–log scale); a best fit is achieved using an order of 2 and 1.9 in $[A_1]_0$ at 100 and 110°C, respectively; k_{1A1} equals 3.2×10^{-6} and 1.2×10^{-5} kg^2 s^{-1} mol^{-2} at 100 and 110°C, respectively (—).

aniline of $[A_1]_0 = 0.98$, $[E]_0 = 5.05$ mol kg^{-1}; and $[A_1]_0 = 2.70$, $[E]_0 = 4.16$ mol kg^{-1}, respectively.

The initial kinetic parameter set (rate constants and equilibrium constants) was taken from the optimized set for PGE + aniline.[4] Parameter limits of the equilibrium constants remained in a range corresponding to literature data: from 0.1 to 1.0 kg mol^{-1}.[19,25] Although the temperature dependencies of $\Delta_r C_{p,\text{prim}}$ and $\Delta_r C_{p,\text{sec}}$ obtained for the model system will be retained, their values at 298.15 K [*a* and *b* in eq. (5)] were changed to accommodate for the higher reaction heat capacity of DGEBA + aniline at different mixture compositions.[5]

Optimized parameters. The optimized parameter set, obtained by the least sum of squares between the simulated and experimental trends in the nonreversing heat flow and heat capacity from MTDSC, is given in Table I together with those parameters obtained for the model PGE + aniline system. Rate constants at 100°C are compared in Table II and show that the DGEBA + aniline system is more reactive than the PGE + aniline system. The higher reactivity increase of the secondary amine–epoxy reaction results in an almost absent substitution effect for the former system ($k_{2OH}/k_{1OH} = 0.43$ at 100°C, as was also observed in Charlesworth[26]). Because PGE and DGEBA have very similar chemical structures, no reactivity difference is expected *a priori*. It has to be noted, though, that whereas the commercial product DGEBA Epon 825 is stated to be a pure grade having a unique chemical structure, GPC measurements showed the presence of a low molecular weight additive (see experimental section). This component is probably added for processing reasons (lower viscosity) and an effect on the reactivity of the epoxy cannot be excluded *a priori*. In another study, DGEBA was purified.[27] Using the op-

TABLE I
Optimized Parameters for the Reaction DGEBA + Aniline[a]

Kinetic parameters (kg mol^{-1} s^{-1})											
k_{1A1}		k_{1OH}		k_{2OH}		Equilibrium constant K_i (kg mol^{-1})					$\Delta_r C_p$ (J mol^{-1}K^{-1})
E_{1A1}	log A_{1A1}	E_{1OH}	log A_{1OH}	E_{2OH}	log A_{2OH}	EOH	A1OH	EA1	EtOH	EtA1	*a*/*b*
79.6	7.5	48.0	4.4	48.4	4.1	0.20	0.50	0.18	0.55	0.18	18.0/19.6
Parameters obtained for DGEBA + aniline											
72.3	6.1	50.4	4.4	52.2	3.9	0.36	0.22	0.28	0.22	0.22	16.1/12.6

[a] Uses the mechanism of Scheme 1: kinetic (*k*) and equilibrium (*K*) parameter set and $\Delta_r C_p$ parameters *a* and *b* from eq. (4); the parameters for the model PGE + aniline are given for comparison[4]; activation energies (*E*) are in kJ mol^{-1}; preexponential factors (*A*) are in kg mol^{-1} s^{-1}.

TABLE II
Comparison Between the Values of the Rate Constants (k) at 100°C for DGEBA + Aniline and PGE + Aniline[a]

Compound	k_{1A1}	k_{1OH}	k_{2OH}	Reactivity ratio ($\approx k_{2OH}/k_{1OH}$)
DGEBA + aniline	2.3	47	20	0.43
PGE + aniline	0.9	22	3.9	0.18

[a] From Ref. 4; k in 10^{-4} kg mol^{-1} s^{-1}.

timized parameters of Table I and the appropriate concentrations of epoxy and amine functionalities, the experimental heat flow of DGEBA + aniline at 400 K from Flammersheim[27] is well predicted. The low molecular weight additive is therefore considered to have no influence on the optimized kinetic parameter set.

The rate of the different reaction steps in Scheme 1 can be simulated along the reaction path (increasing conversion) with the parameter set in Table I (simulation is shown in the second part of this series[11]). The reaction of the primary amine with an epoxy–amine complex initiates the reaction, whereas the reactions of amines with an epoxy–hydroxyl complex take over after these initial stages (2% epoxy conversion at 100°C). The competition between the primary amine and secondary amine for reaction with epoxy functionalities occurs from around 50% epoxy conversion. Note that the relative importance of the different reaction steps as a function of conversion is comparable to the situation in the PGE + aniline system.[4]

Simulation of experimental trends

Concentration profiles as obtained from FT-Raman spectroscopy can be adequately simulated using the optimized parameter set from Table I (see Fig. 4). Although empirical approaches are limited to describing the global conversion evolutions,[28,29] the proposed mechanistic kinetic model contains detailed information about the changing functional groups during reaction. The combination of the "global" epoxy conversion as obtained from the nonreversing heat flow signal [eq. (2)] and the "resolved" conversion present in the heat capacity change [eq. (5)] therefore contains sufficient restrictions to account for effects that could be obtained only by spectroscopic techniques in the past.

Further simulation examples in this section focus on the MTDSC signals and the additional chemorheological information contained in the heat capacity signal when vitrification interferes.[24]

The nonreversing (NR) heat flow in nonisothermal conditions is perfectly predicted for the three heating

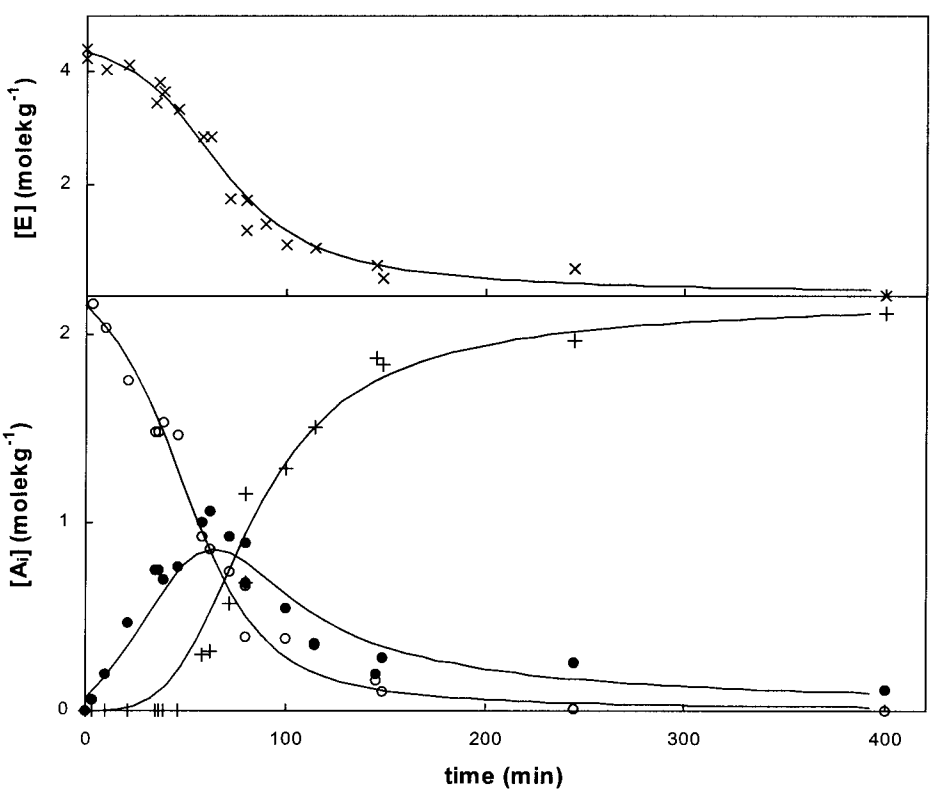

Figure 4 Evolution of the concentration of epoxy [E] (×), primary amine (aniline) [A_1] (○), secondary amine [A_2] (●), and tertiary amine [A_3] (+) as measured by FT-Raman for a stoichiometric DGEBA + aniline mixture cured at 100°C; simulation using the parameter set of Table I (—).

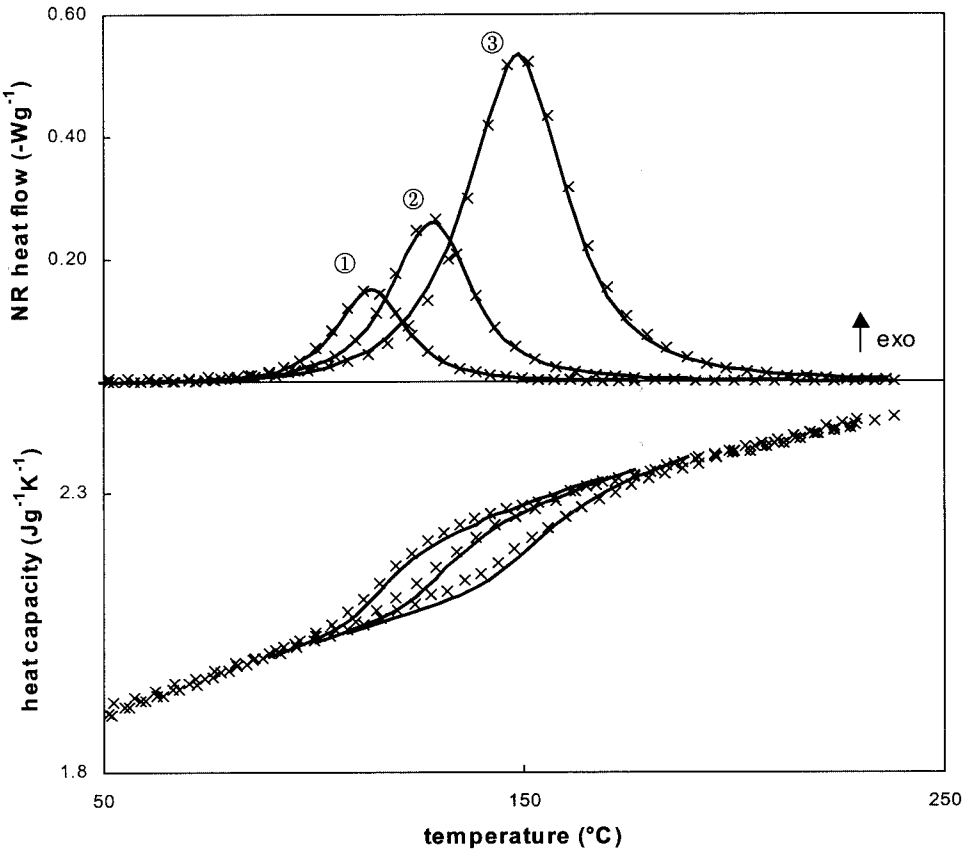

Figure 5 Nonreversing (NR) heat flow and heat capacity during nonisothermal cure of a stoichiometric DGEBA + aniline mixture at 0.5°C/min (①), 1°C/min (②), and 2.5°C/min (③); simulation using the parameter set of Table I (—) and experimental points from MTDSC (symbols).

rates included in Figure 5. Increasing the heating rate results in a shift in the heat flow maximum to higher temperatures. The reaction enthalpy determined by numerical integration is around -107 kJ mol^{-1}, indicating reaction completion in all conditions (see also Fig. 2). The experimental evolutions in heat capacity are also included in Figure 5. The glass transition of the unreacted DGEBA + aniline is outside the scale of this figure ($T_{g0} = -40$°C). The stepwise increase in C_p expresses the higher heat capacities of the products compared to those of the reactants.[5] Simulation of this reaction heat capacity confirms this statement. When one considers that the temperature dependency of $\Delta_r C_{p,\text{prim}}$ and $\Delta_r C_{p,\text{sec}}$ was determined in a temperature range from 25 to 100°C,[5] the close fit indicates that extrapolation to higher temperatures is permitted (the lowest temperature where reaction sets in is 100°C for cure at 0.5°C/min; Fig. 5, ①). Moreover, given that eq. (4) was developed for the model system PGE + aniline, extension to other diglycidyl-type epoxies reacted with aniline seems to be valid. Only the offset values (a and b) of $\Delta_r C_{p,\text{prim}}$ and $\Delta_r C_{p,\text{sec}}$ had to be changed.

An indication for the difference between $\Delta_r C_{p,\text{prim}}$ and $\Delta_r C_{p,\text{sec}}$ can also be obtained by comparing the temperature at which 50% epoxy conversion is reached (from the NR heat flow) with the position of this temperature on the heat capacity evolution. Because these points occur before the midpoint in the stepwise C_p changes, $\Delta_r C_{p,\text{prim}}$ must be smaller than $\Delta_r C_{p,\text{sec}}$ in the respective temperature windows. This procedure can be used as a test experiment on a new epoxy–amine system to determine whether the heat capacity evolution will deliver additional, mechanistic information. The absence of a decrease in C_p as a function of temperature indicates that no vitrification occurs in these nonisothermal experiments, even at the lowest heating rate.[7] In the second part of this series,[11] reaction-induced vitrification will be found to occur in these conditions for the network-forming DGEBA + MDA system because of its higher reactivity and higher $T_{g\text{full}}$.

The glass transition, as obtained after the imposed nonisothermal cure schedule, can be measured in a second heating experiment. This T_g corresponds to full cure conditions ($T_{g\text{full}} = 95$°C) and is independent of the heating rate used for curing the sample (not shown).

In contrast, network-forming epoxy–amine systems usually exhibit high glass-transition temperatures, meaning that isothermal cure cannot be performed

in conditions where vitrification is avoided ($T_{cure} < T_{gfull}$).[1] In case T_{cure} would be chosen higher than T_{gfull}, unacceptable thermal stresses would compromise the final properties. Because the fully cured DGEBA + aniline system does not contain crosslinks, a lower T_{gfull} is attained lying in the range of cure temperatures used (T_{cure} from 60 to 110°C, compared to T_{gfull} = 95°C). In this way, it is possible to cure this system above, below, and inside the glass-transition region of the fully cured polymer. Knowledge of the width of this region, rather than only the glass-transition temperature value itself, is therefore crucial in understanding the isothermal cure of this system (see also the section on ΔC_p at T_g and ΔT_g as a function of x and T). Figure 6 depicts cure experiments of stoichiometric DGEBA + aniline mixtures at 100°C (above T_{gfull}), 95°C (inside T_{gfull} region), and 80°C ($<T_{gfull}$). An example of a system cured near the onset of T_{gfull} will also be discussed (90°C).

Optimization of the experimental NR heat flow and C_p curves was performed in the chemically controlled region, where a close correspondence was found between simulation and experiment (Fig. 6). No clear effect in the NR heat flow was seen at the onset of diffusion-controlled reaction (arrow marks the onset, see next paragraph). For a network-forming epoxy–amine and epoxy–anhydride system, the heat flow quickly fell to zero at this onset.[24] The difference between these systems and the DGEBA + aniline systems lies in (i) the conversion at which vitrification starts (x_{vitr}) and (ii) the T_g– x relation. As can be deduced from partial integration of the NR heat flow until the onset of vitrification, x_{vitr} equals 96 and 99% for the cure at 80 and 90°C, respectively, near full cure conditions. An additional decrease in reaction rate at these high conversions will not be visible in the low-intensity tail of the NR heat flow. The second effect that contributes to the absence of a marked decrease in the reaction rate of the NR heat flow is the fact that the T_g increase at high conversions is less steep in comparison to network-forming systems, because no crosslinks are formed in the linearly polymerizing system (elaborated in the section on glass transition, below).[1]

Apart from the NR heat flow and change in heat capacity during isothermal cure, Figure 6 also shows the heat flow phase, which can be used to detect relaxation phenomena during cure.[24] Although the NR heat flow cannot be used to deduce the onset of diffusion control in DGEBA + aniline, the heat capacity and heat flow phase are very well suited for this purpose. When T_g increases above T_{cure}, vitrification takes place and is clearly seen in the experiment at 80°C as a relaxation peak with a maximum at 510 min. The accompanying stepwise decrease in C_p ($\Delta C_{p,vitr}$) expresses the amount of material that freezes in at this temperature. Note that this effect is superimposed on the reaction heat capacity starting from the vitrification onset. The smaller $\Delta C_{p,vitr}$ for cures at 90 and 95°C corresponds to partial vitrification in these conditions. Diffusion-controlled reaction will be elaborated in the network-forming DGEBA + methylenedianiline system where the accompanying decrease in the reaction rate is clearly present (second part of this series).[11]

Finally, the reliability of the proposed model can be further confirmed by simulating the effect of a change in mixture composition. An increase in the reaction rate for higher initial concentrations of A_1 (higher r) is predicted by the mechanistic model for both the NR heat flow and C_p signals in Figure 7. The lower value of $\Delta_r C_{p,prim}$ compared to $\Delta_r C_{p,sec}$ at 100°C becomes clear when $\Delta_r C_p$ is calculated per mole of the minority component: 28 J mol^{-1} K^{-1} for both r = 1 and r = 0.7 and 26 J mol^{-1} K^{-1} for r = 1.3 at 100°C.[5]

Thermal properties as a function of conversion and composition

Glass transition

T_g as a function of conversion. The epoxy conversion x is used in T_g– x relationships because the epoxide group is involved in both the primary and secondary amine–epoxy reactions and therefore constitutes a measure of the global reaction advancement.[1] Moreover, x can be easily obtained from nonisothermal (MT)DSC measurements subsequent to a certain cure or, more directly, by using the cure experiment itself. When the former method is used, additional reaction advancement beyond 95% is difficult to measure because of the small residual reaction exothermicity and baseline instabilities in nonisothermal conditions. Therefore, the latter method is selected here: the conversion–time relation is determined from partial integration of the isothermal NR heat flow signal from MTDSC as a function of time (see, e.g., Fig. 6 for T_{cure} = 100°C). Considering that the full cure glass transition (T_{gfull}) of the stoichiometric DGEBA + aniline system is around 95°C, a cure temperature of 100°C was used at different cure times to cover the entire conversion range needed for the T_g– x relation. Higher cure temperatures would increase the initial conversion before the first stable data point.

The concentrations of other functional groups can be simulated by using the mechanistic model in Scheme 1 together with the optimized parameter set of Table I (illustrated in Fig. 4). In this way, conversions can be defined on the basis of the consumption of the primary amine (x_{A1}) or the production of the tertiary amine (x_{A3}) [cf. eq. (2)]:

$$x_{A1} = \frac{[A_1]_0 - [A_1]}{[A_1]_0} \quad \text{and} \quad x_{A3} = \frac{[A_3]}{[A_3]_{end}} \qquad (8)$$

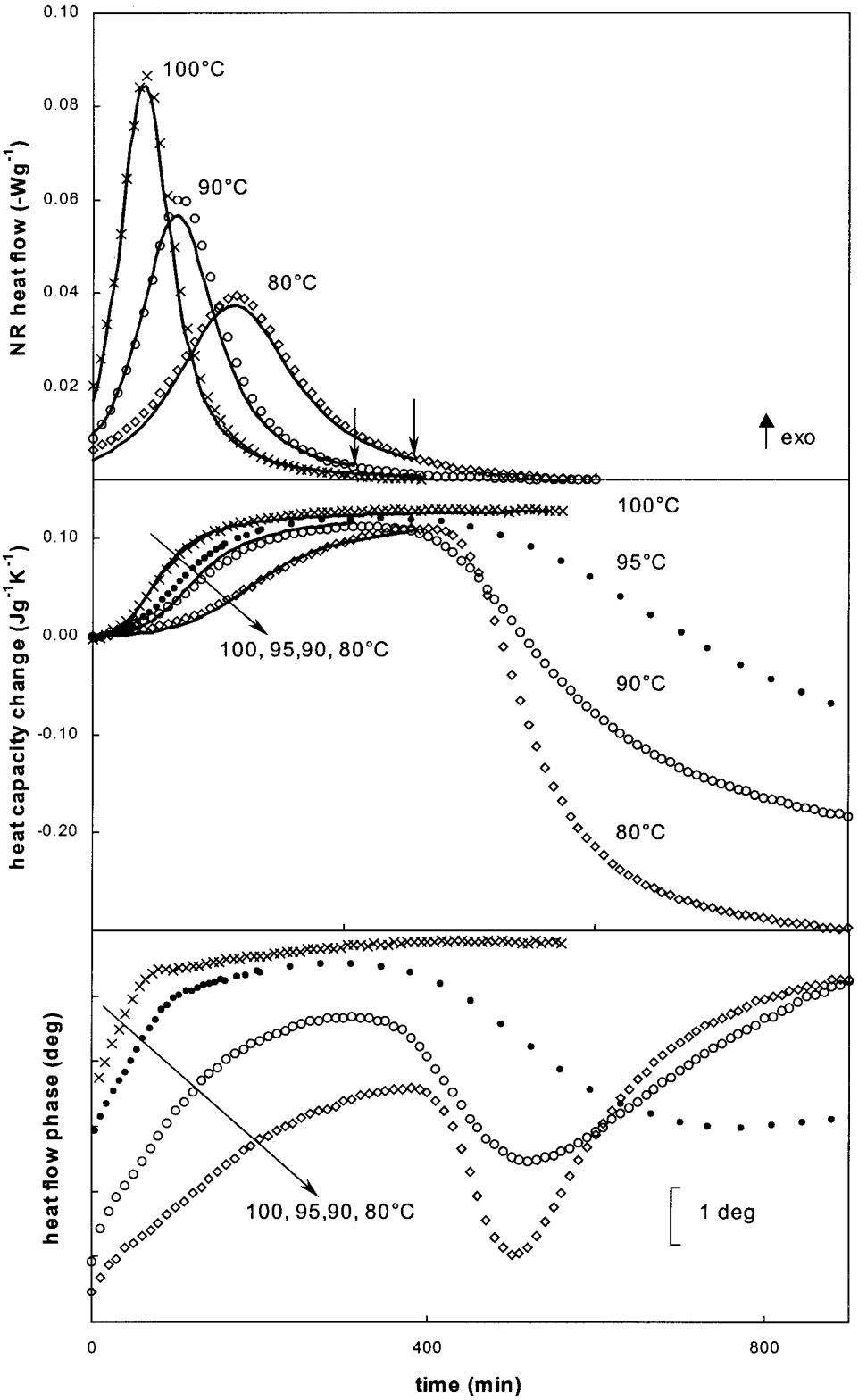

Figure 6 Nonreversing (NR) heat flow, heat capacity change, and heat flow phase for the isothermal cure of stoichiometric DGEBA + aniline mixtures at 80 (◇), 90 (○), 95 (●, NR heat flow not shown), and 100°C (×); simulations of NR heat flow and ΔC_p for cure at 80, 90, and 100°C are depicted using the parameter set of Table I (—); the onset of diffusion-controlled reaction is indicated with an arrow for cure at 90 and 80°C.

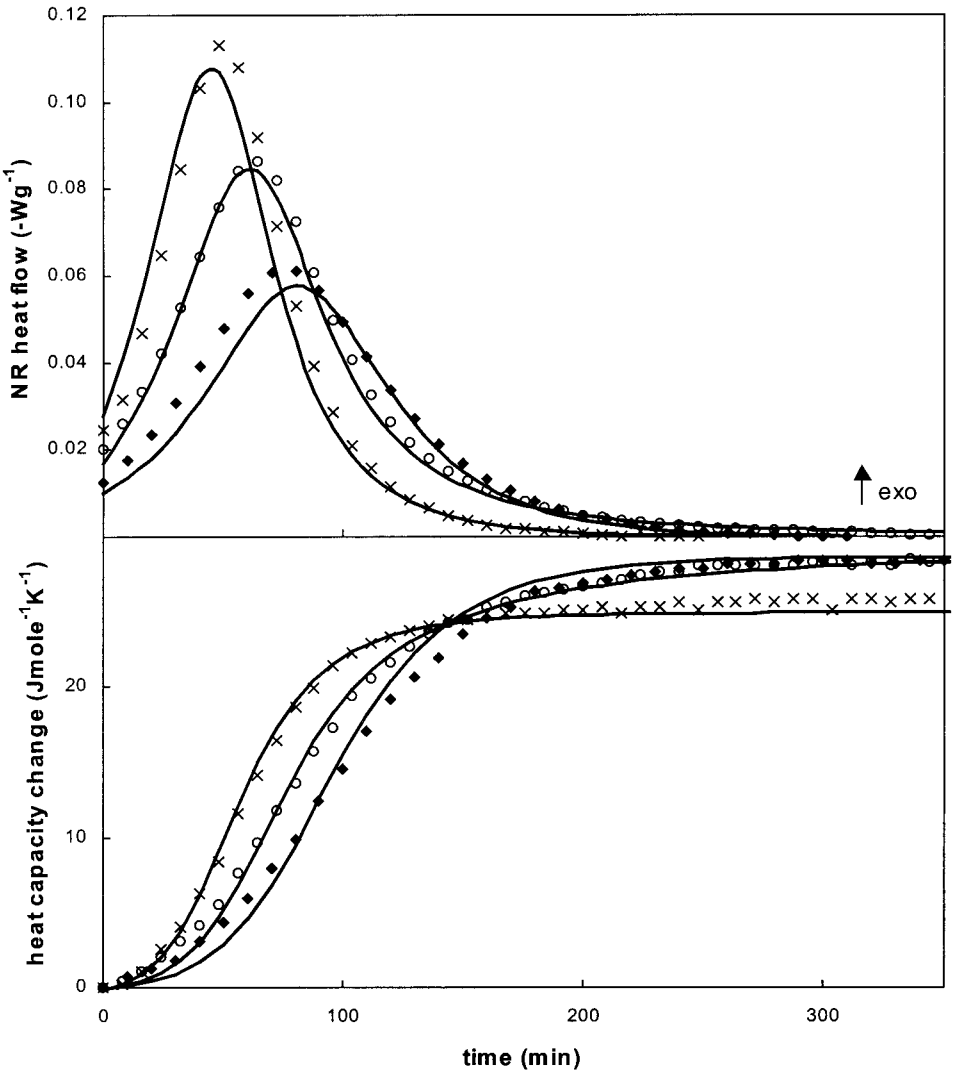

Figure 7 Nonreversing (NR) heat flow and heat capacity change for the DGEBA + aniline cure at 100°C for mixtures of different compositions: $r = 1.3$ (×), $r = 1.0$ (○), and $r = 0.7$ (◆); simulations using the parameter set of Table I (—).

Note that $[A_3]_{end} = [A_1]_0$ for stoichiometric and excess epoxy reactive mixtures.

Figure 8 depicts the relation between T_g and the conversions x, x_{A1}, and x_{A3} for the stoichiometric DGEBA + aniline system cured at 100°C for different cure times. The Couchman relation [eq. (1)], using the measured thermal properties of the unreacted and fully reacted material, does not fit the experimental points perfectly. This relation was formulated on the basis of the epoxy conversion and makes the following assumptions: (i) a random mixture of unreacted segments with fraction $1 - x$ and associated $T_g = T_{g0}$ and reacted segments with fraction x and associated $T_g = T_{gfull}$ exists at conversion x[13] and (ii) the difference in the extrapolated value of the heat capacity between the liquid (or rubbery) state (C_{pl}) and the glassy state (C_{pg}) is assumed to be temperature independent and thus equal to $\Delta C_p(T_g)$ in the range from $T_{g0}(x = 0)$ to $T_{gfull}(x = 1)$.[12]

The first assumption is tentative because, during step-growth polymerization, the monomer is consumed in its early stages, whereas the fully reacted material is formed only in the final stages of reaction.[30] A closer fit of the final stages can be obtained, for example, by using the tertiary amine concentration as a probe for the final material (Fig. 8, ◆, x_{A3}). Further research on other epoxy–amine systems has to elucidate whether an equation that combines conversions of different functional groups can prove to be a better fit for the experimental data.

The second assumption used in the Couchman equation is not valid either for the DGEBA + aniline system (indicated later in the section on ΔC_p at T_g and ΔT_g as a function of x and T; see Fig. 13 below).

Given that x can be easily obtained experimentally, a corrected Couchman equation based on x will be used to fit the relation between T_g and x:

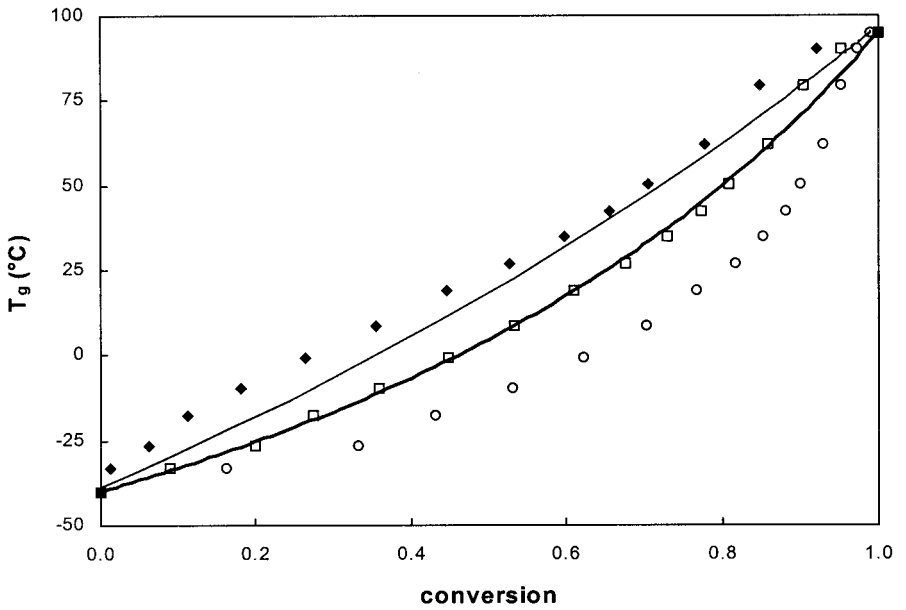

Figure 8 Glass transition (T_g) as a function of: the epoxy conversion (x, □); the conversion based on primary amine groups (x_{A1}, ○); and the conversion based on tertiary amine groups (x_{A3}, ◆) for a stoichiometric mixture of DGEBA + aniline, cured at 100°C for different cure times; the Couchman relation [eq. (1)] is shown by using the measured thermal properties: T_{g0} = 233 K, T_{gfull} = 368 K, and $\Delta C_{pfull}/\Delta C_{p0}$ = 0.97 (thin line); the corrected Couchman relation [eq. (9)] with λ = 0.62 corresponds to the best fit of the relation between T_g and the epoxy conversion x (thick line).

$$\ln(T_g) = \frac{(1-x)\ln(T_{g0}) + \lambda \dfrac{\Delta C_{pfull}}{\Delta C_{p0}} x \ln(T_{gfull})}{(1-x) + \lambda \dfrac{\Delta C_{pfull}}{\Delta C_{p0}} x} \quad (9)$$

where λ is a correction factor, which equals 0.62 for the stoichiometric DGEBA + aniline system (Fig. 8).

Other T_g– x relations based either on thermodynamic considerations [such as eq. (1)] or on structural features of the molecular architecture have been discussed extensively.[13,31–34] In most cases, fitting these equations to the experimental T_g– x data requires one or more adjustable parameters. The selection for eq. (9) in this work is justified by the flexibility of the Couchman equation (λ = 1) to predict the T_g–composition relation for polymer blends.[12] In this way, eq. (9) can be used to obtain information about the composition of coexisting phases during reaction-induced phase separation of thermoplastic modified epoxy–amine systems.[35]

T_g *as a function of molecular weight.* The bifunctionality of both DGEBA and aniline results in the formation of a linear, nonbranched chain. According to the step-growth polymerization mechanism characterizing this epoxy–amine system, the molecular weight will rise sharply to its highest value at the end of the reaction.[30] This can be illustrated by performing a GPC analysis on the samples cured in MTDSC for different times at 100°C: in the last 5% of the reaction an increase in number-average molecular weight (M_n) from 2000 to 13,000 g/mol was obtained. The classical model for the effect of molecular weight on T_g can be used[36,37]:

$$T_g = T_{gfull} - \frac{K}{M_n} \quad (10)$$

where K is a constant. The fact that a close correspondence is found in Figure 9 indicates that the increase in M_n, which results in a decrease in the concentration of chain ends, determines the glass transition of this linearly polymerizing system.

T_g *as a function of* r. Slight stoichiometric imbalances significantly limit the attainable molecular weight values for polymerizations exhibiting the step-growth mechanism.[30] The effect on the full cure glass transition (T_{gfull}) of large imbalances in the reactant ratio r, defined as the ratio of NH to oxirane functionalities, is depicted in Figure 10. Lower values of T_{gfull} are found when r differs from one, both for excess epoxy ($r < 1$) and for excess amine ($r > 1$) mixtures. To compare T_{gfull} values for all these mixtures in a straightforward way, the reactant ratio for excess amine mixtures should be redefined ($r' = 1/r$) to be also less than or equal to one (Fig. 10, ●).

Thus, the same imbalances in epoxy or amine functionalities result in the same, lower molecular weight values as indicated by the coinciding T_{gfull} trends.

ΔC_p at T_g and ΔT_g as a function of x and T

To understand the evolution of $\Delta C_p(T_g)$ with x, the effect of x on the heat capacity in the liquid (C_{pl}) and

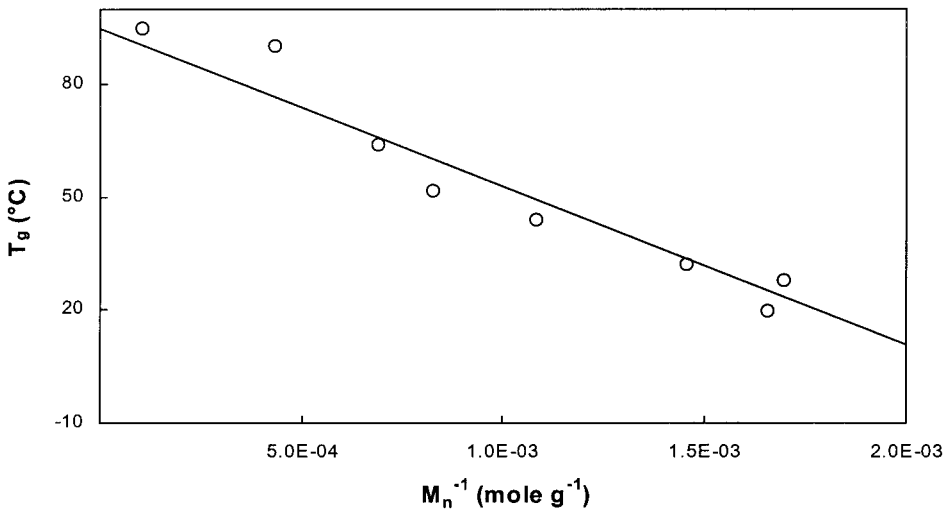

Figure 9 T_g (from MTDSC) as a function of the reciprocal of M_n (from GPC) for a stoichiometric mixture of DGEBA + aniline, cured at 100°C for different cure times (○); eq. (10) relates these two quantities using $K = 4.2 \times 10^4$ g mol^{-1} K^{-1} (line).

glassy state (C_{pg}) must be determined first. As already elaborated for the model system PGE + aniline, and as was depicted for DGEBA + aniline in Figure 6, a positive reaction heat capacity ($\Delta_r C_p$), increasing with cure temperature, is present for these systems in the liquid state, indicating that C_{pl} of the reaction products is higher than that of the reactants.[5] $\Delta_r C_p$ at 100°C, for example, is 0.13 J g^{-1} K^{-1} for DGEBA + aniline. The effect of conversion on C_{pg} was obtained by measuring the heat capacity at −60°C after consecutive nonisothermal experiments up to 100°C. A certain reaction advancement occurs in each experiment. Using the T_g as determined from the heat capacity signal, these intermittent conversions were obtained from the corrected Couchman relation [eq. (9); Fig. 8]. Figure 11 indicates a decrease in C_{pg} starting from a conversion around 30% (T_g = −18°C) and amounting to about 0.07 J g^{-1} K^{-1} at the reaction completion. This can be ascribed to a decrease in free volume as the molecular weight increases, thus decreasing the contribution of molecular modes in the glassy state.[38]

Considering the diverging evolutions in C_{pl} and C_{pg} with conversion, an increase of $\Delta C_p(T_g)$ with x would be expected. Although an initial increase is seen in

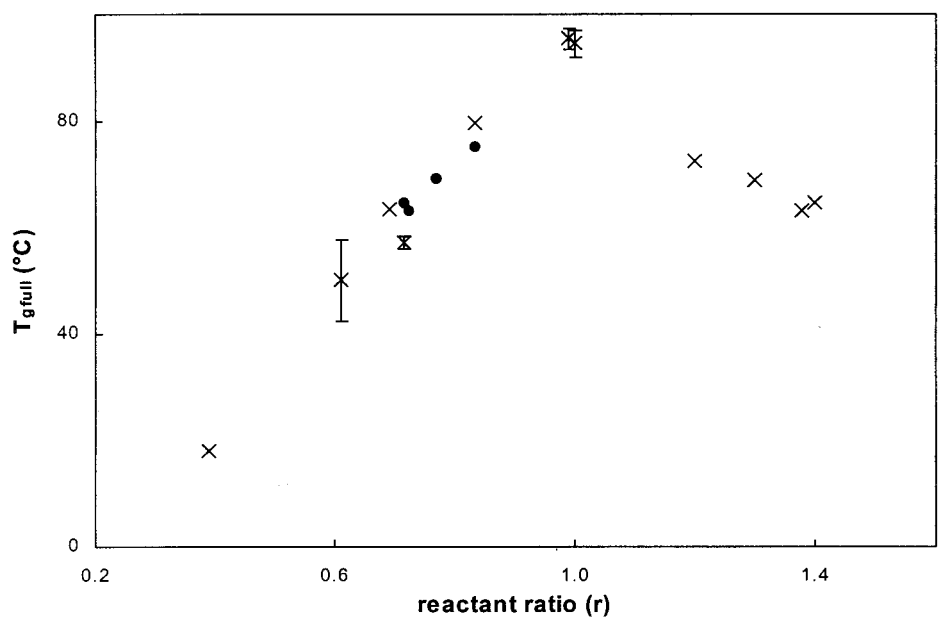

Figure 10 Full cure glass transition as a function of reactant ratio (r) for DGEBA + aniline (×); redefined reactant ratio ($r' = 1/r$) for $r > 1$ (●); error bars are included when more than two measurements were averaged.

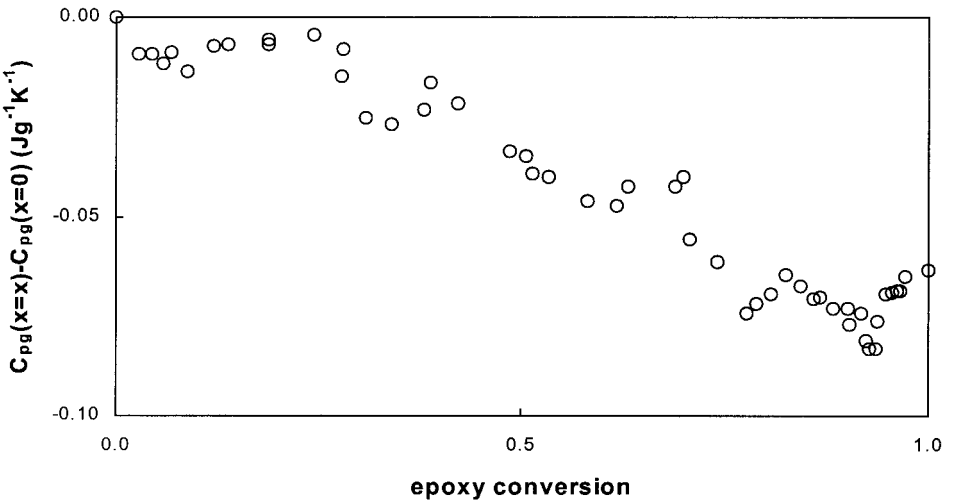

Figure 11 Difference between the heat capacity in the glassy state for the stoichiometric DGEBA + aniline mixture at −60°C after a certain conversion, $C_{pg}(x = x, T = -60°C)$, and for a fresh mixture, $C_{pg}(x = 0, T = -60°C)$, as a function of x.

Figure 12 until about 20% conversion, $\Delta C_p(T_g)$ decreases beyond this point until the fully cured state is reached. As indicated in Figure 13 for the unreacted and fully reacted system, this can be ascribed to the fact that the temperature dependency of C_{pg} is greater than that of C_{pl}, resulting in the observed converging trend after 20%.[39] Using the fragility terminology introduced by Angell, a net evolution to a stronger liquid was observed.[40] The assumption used to derive the Couchman eq. (1) (see the section on glass transition), stating that $\Delta C_p = C_{pl} - C_{pg}$ is temperature independent and thus equal to $\Delta C_p(T_g)$, is therefore invalid or at least too rough an approximation, which justifies the need for the correction factor λ in eq. (9).

Figure 13 uses the information on $C_{pg}(x, T)$ (○) to illustrate the evolution of $\Delta C_p(T_g)$ with conversion further (–).

The evolution of $\Delta C_p(T_g)$ with conversion is important for calculating the mobility factor for highly reactive epoxy–amine systems where vitrification interferes.[7] This is discussed in the second part of this series.[11]

A measure for the width of the glass-transition region ΔT_g was obtained from the derivative of C_p to temperature as a function of temperature. ΔT_g is defined in this work as the width at half-height of the resulting peak.[41] Using the same experimental approach as used for $\Delta C_p(T_g)$, the conversion corresponding to ΔT_g can be determined from T_g. An increase in broadness is seen in Figure 14, in agreement with an increase in polydispersity for the linear step-growth polymerization.[30] The decrease in the final stages of reaction could be related to the fact that when 100% conversion is reached, no lower molecular

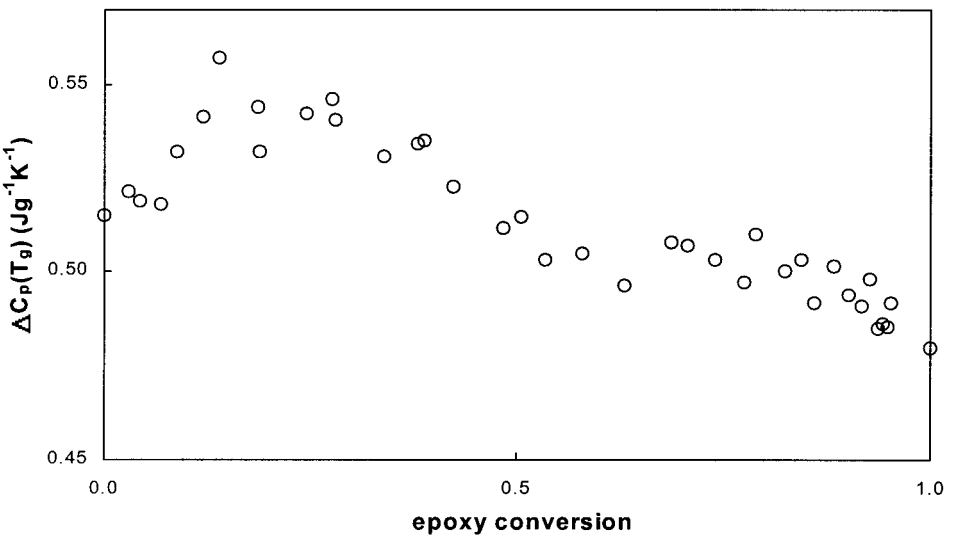

Figure 12 Heat capacity change at T_g [$\Delta C_p(T_g)$] as a function of x as obtained from the heat capacity signal of MTDSC in nonisothermal postcure experiments.

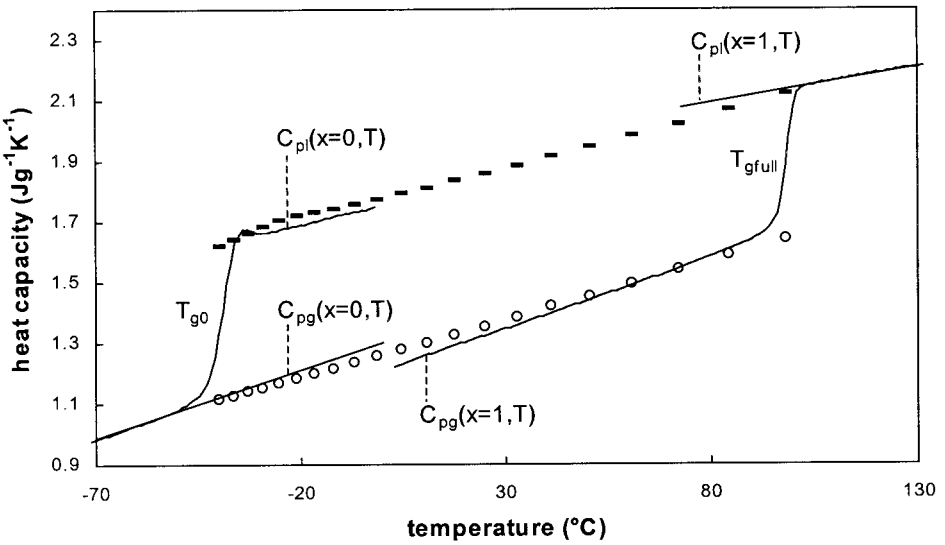

Figure 13 Heat capacity as a function of temperature for an unreacted and fully reacted stoichiometric DGEBA + aniline mixture (—); C_{pg} (○): effect of x as obtained from Figure 11 and temperature dependency from $C_{pg}(x = 0, T)$; C_{pl} (–), from the experimental $\Delta C_p(T_g)$ in Figure 12.

weight components that could act as plasticizer remain. Thus, the evolution of ΔT_g with conversion is more complex than that of the polydispersity. The width of T_g is important in understanding partial vitrification phenomena that were elaborated earlier.

CONCLUSIONS

The stepwise decrease in the heat capacity signal accompanied by a relaxation peak in the heat flow phase signal during the final stages of the DGEBA + aniline reaction corresponds to reaction-induced vitrification. No decrease in reaction rate, however, can be detected in the nonreversing heat flow at these high conversions ($x_{vitr} > 95\%$ for T_{cure} ranging from 80 to 95°C). A mechanistic model including both reactive and nonreactive equilibrium complexes in combination with the predominant reaction steps was proposed for the chemically controlled reaction ($x < x_{vitr}$). Although the epoxy–amine complex initiates the reaction with primary amine, the reaction of the epoxy–hydroxyl complex with primary and secondary amine groups dominates beyond these initial stages.

The input used for the optimization of the kinetic parameters is the global conversion extracted from the nonreversing heat flow and the resolved conversion from the heat capacity signal. The optimum kinetic parameter set is able to simulate both isothermal and

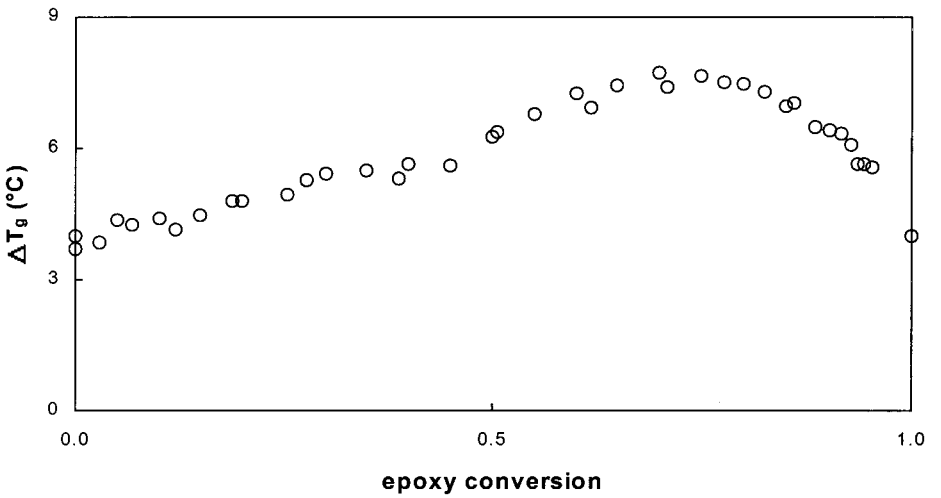

Figure 14 Width of the glass-transition region ΔT_g, determined at the half-height of the derivative of the heat capacity signal in nonisothermal conditions, as a function of conversion.

nonisothermal experiments for both signals from MTDSC. Moreover, the concentration profiles for E, A_1, A_2, and A_3, as obtained by Raman spectroscopy, can also be predicted, thus confirming the validity of the mechanistic approach and again pointing out the detailed additional information provided by the heat capacity signal. Note that the same reaction mechanism was successfully used for the model epoxy–amine PGE + aniline system using kinetic parameters that account for its lower reactivity.[4] The presented modeling approach is thus not only able to predict changes in reaction rate attributed to cure temperature and mixture composition, but it can also incorporate a change in epoxy chemistry. The kinetic model promises to be a general tool to predict changes in concentrations of functional groups during cure of epoxy–amine systems.

The epoxy conversion (x) can be related to the evolving thermal properties of the linearly polymerizing DGEBA + aniline: T_g, heat capacity change at T_g [$\Delta C_p(T_g)$], and width of the glass-transition region (ΔT_g). The Couchman equation, based on thermodynamic considerations, must be corrected to fit the experimentally obtained T_g– x relation. The need for a correction can be attributed to invalid assumptions (for DGEBA + aniline) made in the Couchman equation. First, postulating that a mixture of unreacted groups with fraction $(1 - x)$ and $T_g = T_{g0}$ and of reacted groups with fraction x and $T_g = T_{g\text{full}}$ exists at conversion x is invalid during step-growth polymerization of DGEBA + aniline. The conversion based on the tertiary amine groups (A_3), as can be obtained from the simulation of its concentration profile, is a better probe for the fraction of fully reacted material. Second, assuming a temperature-independent $\Delta C_p = C_{\text{pl}} - C_{\text{pg}}$ equal to $\Delta C_p(T_g)$ turns out to be incorrect.

When the molecular weight instead of x is used, a simple relationship is found, indicating that the decrease in concentration of chain ends determines the increase in T_g for an increase in molecular weight. The mixture composition has to be controlled with care because large molecular weight depressions resulting from stoichiometric imbalances decrease T_g. An indication for the evolving molecular weight distribution during the linear polymerization can be obtained from ΔT_g– x plots. The evolution of $\Delta C_p(T_g)$ with x shows a maximum at 20% conversion attributed to (i) positive contributions from the increasing reaction heat capacity ($\Delta_r C_p$) and the decreasing heat capacity in the glassy state with conversion and (ii) a negative contribution attributed to the higher slope in the temperature dependency of the heat capacity in the glassy state compared to that of the liquid state. Using the fragility approach, a net evolution toward a stronger liquid was found.

In the second part of this series,[11] the effect of the epoxy–amine chemistry on the reaction kinetics and thermal properties is further investigated by considering a network-forming system in which vitrification has profound effects on the reaction rate in the later stages of reaction.

The work of S. Swier was supported by grants of the Flemish Institute for the Promotion of Scientific-Technological Research in Industry (I.W.T.).

References

1. Gillham, J. K.; Enns, J. B. Trends Polym Sci 1994, 2, 406.
2. Kamal, M. R. Polym Eng Sci 1974, 14, 231.
3. Vyazovkin, S.; Sbirrazzuoli, N. Macromolecules 1996, 29, 1867.
4. Swier, S.; Van Mele, B. Thermochim Acta, to appear.
5. Swier, S.; Van Mele, B. J Polym Sci Part B: Polym Phys 2003, 41, 594.
6. Oleinik, E. F. Adv Polym Sci 1986, 80, 49.
7. Van Assche, G.; Van Hemelrijck, A.; Rahier, H.; Van Mele, B. Thermochim Acta 1996, 286, 209.
8. Reading, M. Trends Polym. Sci., 8, 248 (1993).
9. Plazek, D. J.; Frund, Z. N. J Polym Sci Part B: Polym Phys 1990, 28, 431.
10. Van Assche, G.; Van Hemelrijck, A.; Rahier, H.; Van Mele, B. Thermochim Acta 1995, 268, 121.
11. Swier, S.; Van Assche, G.; Van Mele, B. J Appl Polym Sci 2004, 91, 2814.
12. Couchman, P. R.; Karasz, F. E. Macromolecules 1978, 11, 117.
13. Venditti, R. A.; Gillham, J. K. J Appl Polym Sci 1997, 64, 3.
14. Shell Method HC-427-81: Perchloric acid method.
15. Gaur, U.; Wunderlich, B. J Phys Chem Ref Data 1982, 11, 313.
16. Van Assche, G.; Van Hemelrijck, A.; Van Mele, B. J Therm Anal Calorim 1997, 49, 443.
17. Flory, P. J. Principles of Polymer Chemistry; Cornell University Press: Ithaca, NY, 1953.
18. Mijovic, J.; Fishbain, A.; Wijaya, J. Macromolecules 1992, 25, 979.
19. Rozenberg, B. A. Adv Polym Sci 1986, 75, 113.
20. Lyon, R. E.; Chike, K. E.; Angel, S. M. J Appl Polym Sci 1994, 53, 1805.
21. deBakker, C. J.; George, G. A.; St John, N. A.; Fredericks, P. M. Spectrochim Acta 1993, 49A, 739.
22. Dollish, F. R.; Fateley, W. G.; Bentley, F. F. Characteristic Raman Frequencies of Organic Compounds; Wiley: New York, 1974.
23. van Overbeke, E.; Carlier, V.; Devaux, J.; Carter, J. T.; McGrail, P. T.; Legras, R. Polymer 2000, 41, 8241.
24. Van Assche, G.; Van Hemelrijck, A.; Rahier, H.; Van Mele, B. Thermochim Acta 1997, 304/305, 317.
25. Enikolopiyan, N. S. Pure Appl Chem 1976, 48, 317.
26. Charlesworth, J. M. J Polym Sci Part A: Polym Chem 1987, 25, 731.
27. Flammersheim, H. J. Thermochim Acta 1998, 310, 153.
28. Kamal, M. R. Polym Eng Sci 1974, 14, 231.
29. Vyazovkin, S.; Sbirrazzuoli, N. Macromolecules 1996, 29, 1867.
30. Young, R. J.; Lovell, P. A. Introduction to Polymers; Chapman & Hall: London, 1991; Chapter 2.
31. Van Hemelrijck, A. Ph.D. Thesis, Free University of Brussels, Belgium, 1996.
32. Hale, A.; Macosko, C. W.; Bair, H. E. Macromolecules 1991, 24, 2610.
33. Pascault, J. P.; Williams, R. J. J. J Polym Sci Part B: Polym Phys 1990, 28, 85.
34. DiBenedetto, A. T. J Polym Sci Part B: Polym Phys 1987, 25 1949.
35. Swier, S.; Van Mele, B. Polymer, to appear.
36. Fox, T. G.; Flory, P. J. J Appl Phys 1950, 21, 581.
37. Cowie, J. M. G.; Toporowski, P. M. Eur Polym Mater 1968, 4, 621.
38. Vendetti, R. A.; Gillham, J. K.; Jean, Y. C.; Lou, Y. J Appl Polym Sci 1995, 56, 1207.
39. Stevens, G. C.; Richardson, M. J. Polymer, 24, 851 (1983).
40. Angell, C. A. J Res Natl Inst Stand Technol 1997, 102, 171.
41. Song, M.; Hourston, D. J.; Schafer, F.-U.; Pollock, H. M.; Hammiche, A. Thermochim Acta 1997, 304/305, 335.